Positive Effect of Laser Structured Surfaces on Tribological Performance

Tobias Stark[1], Sabri Alamri[2], Alfredo I. Aguilar-Morales[2], Thomas Kiedrowski[1], Andrés Fabián Lasagni[2, 3]

[1] *Robert Bosch GmbH, Robert-Bosch-Campus 1, 71272 Renningen, Germany*
E-mail: tobiasbenedikt.stark@de.bosch.com
[2] *Fraunhofer-Institut für Werkstoff- und Strahltechnik IWS, Winterbergstr. 28, 01277 Dresden, Germany*
[3] *Institut für Fertigungstechnik, Technische Universität Dresden, George-Bähr-Str. 3c, 01069 Dresden, Germany*

In recent years laser surface structuring has emerged as a viable tool to enhance surface functionality. In this study, an ultrashort pulsed laser is used to create advanced surface structures in order to improve the tribological properties of steels. The objective is to decrease friction and wear especially for the mixed lubrication regime in which body and counterbody are in contact. We state the hypothesis that the high flow resistance in small channels helps to hold the lubricant in the tribocontact and therefore separates contacting asperities. Direct Laser Writing and Direct Laser Interference Patterning methods are used to create cross-like structures of different channel sizes. Tribological properties of these structures are evaluated by means of a ball-on-disc tribometer. The surface structures and the wear behavior are analyzed with confocal microscopy. The results show a decrease of the coefficient of friction depending on the size of the channels. This behavior is discussed and compared to the hypothesis stated above.

DOI: 10.2961/jlmn.2019.01.0003
Keywords: laser surface texturing, surface functionalization, tribology, Direct Laser Interference Patterning (DLIP), Direct Laser Writing (DLW), Stribeck curve, friction

1. Introduction

Tribology is a wide-spread field with various applications. One of the most important application is in the automobile industry. In passenger cars friction occurs in the engine, transmission, tires and brakes. According to Holmberg et al. [1], the direct frictional losses, with braking friction excluded, are 28% of the fuel energy. In total, 21.5% of the fuel energy is used to move the car. Therefore, there is an enormous potential to reduce the global energy consumption by enhancing the tribological performance. There are also other fields of application, e.g. bionic engineering where for example the sandfish's skin which is structured in a way that friction is reduced serves as a model [2].

In a tribological system, friction and wear phenomena occur. In general, the main objective is to increase the wear resistance of the parts in contact as well as to reduce the friction coefficient. These properties depend, besides others, mainly on the topology of the surfaces which are in contact and the operating conditions, including lubrication, temperature, load and relative sliding velocity of the two bodies [3]. Many efforts have been made to enhance the tribological performance by influencing these operating conditions. The easiest way to decrease friction is to introduce a lubricating medium (oil or grease) with an adequate viscosity-temperature dependence. The properties of these lubricants are also affected by additives [4]. However, the friction and wear behavior can be also controlled by structuring the surface of one of the contacting bodies with a laser [5]. For laser surface structuring, two different methods were applied in this study, namely Direct Laser Writing (DLW) and Direct Laser Interference Patterning (DLIP). The main difference of the two methods is the intensity profile at the working plane as can be seen in Figure 1.

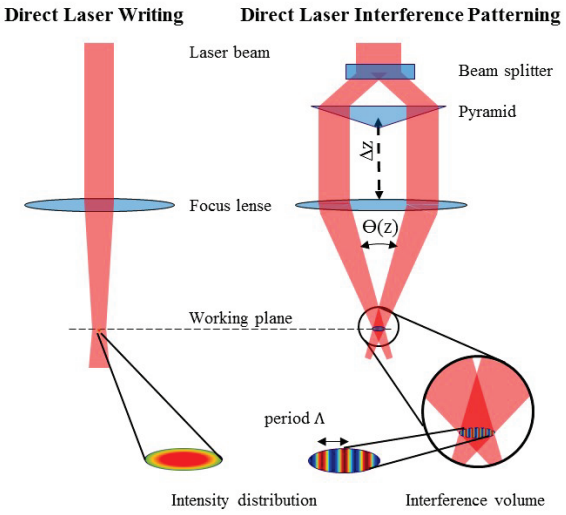

Fig. 1 Comparison of intensity distribution at working plane for DLW and DLIP.

For DLW, one single laser beam with a Gaussian-shaped intensity profile is focused. For DLIP, a single laser beam is divided into two or more coherent beams that interfere with each other. Therefore, due to constructive and destructive interference, a specific intensity pattern is obtained [6]. The

field of applications for DLIP is broad. It ranges from friction reduction on metals, improved cell adhesion for dental implants to wettability control on metals and polymers between others [7-9]. DLIP is also a suitable method to create small surface structures in the sub-micrometer range [10]. The reason why small channel-like structures are preferred is based on a hypothesis which will be introduced in the next section.

In this study, the interference of two laser beams was used which leads to a line-like pattern. By rotating the sample by 90° cross-like patterns can be produced. Aguilar et al. [11] describe the fabrication of the periodic structures on stainless steel. The structures created with DLIP have a periodicity of 4 µm and 8 µm and a depth of around 1 µm.

1.1 Theoretical considerations

The objective of the laser structure in the tribocontact is to increase the amount of oil by building reservoirs. However, if the channels are too large, the oil drains through the channels, as water is displaced for instance in a rain tire (to provide contact between the tire and the street) [12]. As a consequence, there is not enough oil to separate the contacting asperities. The idea behind the small channels is to increase the flow resistance and thereby to avoid the displacement of the oil. This hypothesis is based on a fluid dynamical approach. Generally, the flow resistance is defined as [13]:

$$R_h = \frac{\Delta p}{Q}, \tag{1}$$

where Δp is the pressure difference between two channel ends and Q is the flow rate.

The cross-section of the laser-structured channels is a rather u-shaped one. However, for the reason of simplicity, we assume a rectangular shape where the width w is larger than the height h obtaining a Poiseuille flow problem case. Since no analytical solution is known for this problem, a solution for an adequate Fourier sum with the corresponding boundary conditions can be found. The specific steps are outlined in [13]. From this solution, the velocity field can be determined. As a next step, the velocity field can be integrated to obtain the flow rate Q:

$$Q \approx \frac{h^3 w \Delta p}{12 \eta L}\left[1 - 0.630\frac{h}{w}\right], \text{for } h < w \tag{2}$$

where η is the dynamic viscosity and L the length of the channel. By setting equation (2) into equation (1) and rearranging for R_h, it is possible to see that the flow resistance increases if h and w are small. This means that narrow and shallow channels have a higher resistance for the fluid as wide and deep channels.

In this study, experiments were designed to validate this hypothesis.

1.2 Laser surface texturing and tribology

A significant amount of research in the field of laser surface texturing and tribology has been conducted with closed structures, which are mainly micro-dimples. For instance, Etsion reviewed different concepts that have been utilized [14]. Many research articles state the reduction of the coefficient of friction (COF) depending on the depth, diameter or arrangement of the dimples. One positive effect of dimples is described by cavitation in the diverging gap. The consequence is a positive net pressure build-up which is illustrated by Braun [15]. However, the necessary conditions for cavitation are high relative sliding velocities and simultaneously low pressure. Wahl [16] not only investigated dimples but also open or "inter-communicating" structures. It is important to note that the contacting geometries were built as a conformal contact. Furthermore, the width of the channels lies between 60 µm and 300 µm. The results for dimples show no significant effects for sliding velocities below 0.5 m/s and a reduction of COF for sliding velocities greater than 0.5 m/s. For the open structures, a small increase of COF was shown for the first case whereas a significant increase of COF was shown for the latter case.

A slightly different approach to reduce COF by means of laser surface texturing was reported by the Bonse et al. [17]. They coated different substrate materials with titanium nitride (TiN) and applied a femtosecond laser to create laser-induced periodic surface structures (LIPSS) with sub-wavelength periods ranging between 470 nm and 600 nm. In tribological tests, the COF was determined under reciprocating sliding conditions. However, the reported results showed that friction and wear could not be significantly reduced in comparison to unstructured TiN surfaces.

1.3 Stribeck curve

The Stribeck curve illustrates the different lubrication regimes dependent on the relative sliding velocity between body and counterbody [18]. Figure 2 shows a typical Stribeck curve for a non-conformal contact which occurs for a ball on a disc because the contact is a point contact. For a point contact, the pressure build-up is much lower than for a flat contact since for a point contact the lubricant is displaced in all directions.

As can be seen in Figure 2, there are three lubrication regimes, namely boundary lubrication, mixed lubrication and elasto-hydrodynamic lubrication. The objective of this study is to decrease the COF for the mixed lubrication regime, where both contacting asperities and a separating fluid film occur. Therefore, this regime is prone to have high friction and wear due to the contacting asperities.

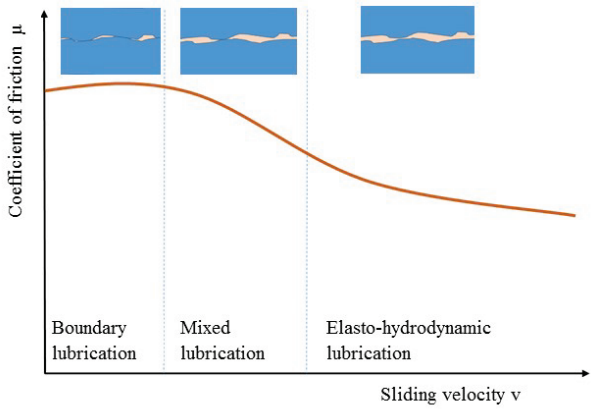

Fig. 2 Stribeck curve for non-conformal contact. Adapted from Gachot et al. [19].

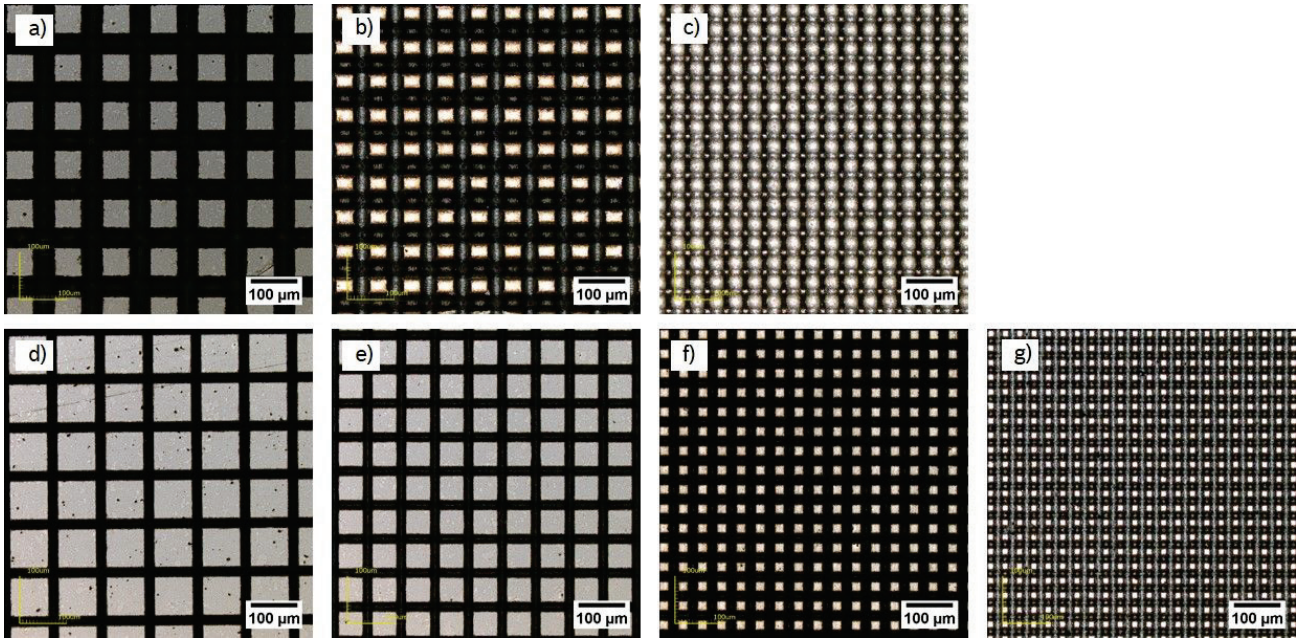

Fig. 3 Channel-like structures created with DLW. a) and d) have a period Λ = 100 µm, for b) and e) Λ = 70 µm, for c) and f) Λ = 40 µm and for g) Λ = 30 µm. a)-c) have a width of 30 µm and d)-g) have a width of 12 µm. The scale bar in each picture marks 100 µm.

2. Materials and methods

2.1 Materials

For the structuring and the tribological experiments, martensitic stainless steel X90CrMoV18 (1.4112) was used. The sheets were cut in rectangular shaped parts of 16 mm x 6 mm in order to fit as samples for the tribometer. The samples were polished by lapping in order to obtain a roughness of R_z = 0.20 µm. Before the tribological characterization, the polished samples were treated with the laser except for the reference sample.

All samples were cleaned using isopropanol in an ultrasonic bath for 10 minutes. Afterwards, the samples were dried and then rinsed with petrolether (boiling temperature 40-60 °C). This procedure was repeated before the laser process and the tribological evaluation.

2.2 Laser surface texturing

For the DLW process, an ultrashort pulsed laser (Trumpf Trumicro 5070 Femto Edition) was used, combined with a scanner installed in a machine (GLcompact from GFH). The laser wavelength is 1030 nm, the pulse length is 900 fs and the repetition rate is 400 kHz. The used laser fluence for the DLW structures was 1.54 J/cm^2 for the wide structures and 0.44 J/cm^2 for the narrow structures.

For the DLIP process, also an ultrashort pulsed laser (Trumpf Trumicro 5x50) was used, with a wavelength of 1030 nm and a pulse length of 6 ps. The repetition rate was in this case 400 kHz. A DLIP optical head (Fraunhofer IWS, Dresden, Germany) is installed to automatically create the interference pattern. The setup of the optical head has been already published elsewhere [20]. The laser fluence for the DLIP structures is 0.55 J/cm^2 for the period of 8 µm and 0.41 J/cm^2 for the period of 4 µm.

2.3 Characterization of tribological properties

For the evaluation of the surface structures, an Anton Paar Tribometer (MCR301) was used. As oil, a Polyalphaolefin (PAO) with a viscosity of 39.5 mm^2/s at 25 °C (operating condition) was used. It is the base oil of the commonly used grease Isoflex Topas L32. This oil has no additives in order to avoid side effects which are not induced by the surface structures. As a tribological counterbody, a 100Cr6 ball with a diameter of 12.7 mm was used.

As a first step, three samples were fixed in the sample holder with an angle of 45° regarding the horizontal plane. Secondly, 1 µl of the PAO was put on each sample with a µl-pipette. Then, the sample holder was fixed on the device and the ball in the ball-holder was placed above the sample. The ballholder was approached to the sample which makes the oil ousted around the tribocontact. Finally, a normal force of 20 N was applied, which corresponds to 4.71 N per sample. When this force is reached, the ball started to rotate and the measurement cycle began. The measurement cycle consisted of 9 Stribeck curves, which were grouped in 3 packages, and three endurance parts at the beginning of the cycle and in between the Stribeck packages. Their purpose is to avoid run-in behavior.

The total normal force always was 20 N and the rotation speed during the endurance parts was 20 rpm which corresponds to a sliding velocity of 0.009 m/s. The Stribeck curves were recorded using a logarithmic ramp up to 1.4 m/s.

2.4 Surface characterization

A Laser Confocal Microscope (Olympus LEXT OLS4000) was used to characterize the surface morphology of the laser treated samples.

3. Results and discussion

3.1 Laser surface texturing

Firstly, DLW was used to fabricate different channel-like structures varying the distance between the channels (period Λ) between 100 µm and 30 µm. Later, channels with two different widths (12 µm and 30 µm) were produced. The narrow channels were processed installing an optical attenuator into the beam path and thus reducing the range of the Gaussian beam profile which lies above the ablation threshold. To control the channel depth, the number of overscans was systematically changed. Using these variables, seven different structures with three different depths each were fabricated as indicated in Table 1. Figure 3 shows an overview of these structures. The shape of the produced structures is a u-shaped one. The width given in Table 1 corresponds to the top width. A typical radius at the bottom of the channel is between 3-5 µm.

Since the structure size which can be obtained by DLW is limited by the spot size at the focal position, DLIP method was used to create cross-like structures, but with significantly smaller spatial periods Λ (smaller than 10 µm). Precisely, cross-like structures with Λ = 8 µm and Λ = 4 µm were fabricated. Figure 4 illustrates examples of these patterns. The structure depth for these patterns was 0.96 µm and 0.79 µm, respectively.

Table 1 Overview of the structures created with DLW

Period Λ (µm)	Channel depths (µm)	Channel width (µm)
100	4, 12, 24	30
70	4, 12, 24	30
40	4, 12, 24	30
100	3, 6, 9	12
70	3, 6, 9	12
40	3, 6, 9	12
30	3, 6, 9	12

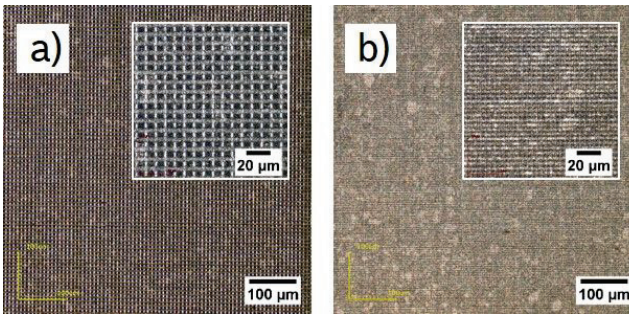

Fig. 4 Cross-like structures fabricated using DLIP with spatial periods of a) Λ = 8 µm and b) Λ = 4 µm.

3.2 Evaluation of tribological performance

From the measurement cycle described in section 2, the Stribeck curves for all treated samples were extracted and its mean value and standard deviation of the COF were determined. Figure 5 shows these values against the sliding velocity v_s, yielding in a typical Stribeck curve. The different curves in Figure 5a represent three different depths (4 µm, 12 µm and 24 µm) for the case of wide (30 µm width) and a spatial period Λ of 100 µm, compared to a polished reference sample. In figure 5b, three different depths (3 µm, 6 µm and 9 µm) were evaluated, for the case of a spatial period Λ of 30 µm and narrow channels (12 µm width), which were also compared to the same polished reference sample. The grey areas in Figure 5a and 5b between the lowest and the highest Stribeck curve for low sliding velocities v_s mark the range of COF for the mixed lubrication regime for the structured samples in both cases (narrow and wide structures). Both the extension of the range and its absolute level are significantly (~20%) lower for the case of many narrow channels. As it can be observed, for all displayed images, it was possible to reduce the COF, especially for sliding speeds below 10^{-2} m/s. In particular, for the narrow channels (Λ = 30 µm), the reduction of the COF was better than for the samples with large distances between the channels (Λ = 100 µm).

Another important observation is related to the structure depth. While for the large patterns (Figure 5a) the depth strongly influenced the COF (for sliding speeds below 10^{-2} m/s), this was not the case for the textures with 30 µm period (Figure 5b). In addition, the best performance for the large structures was observed for the sample showing a depth of 4 µm.

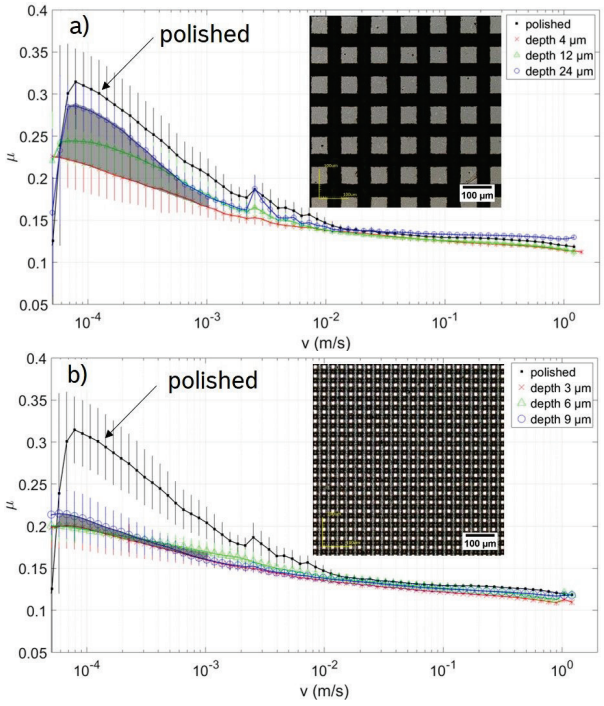

Fig. 5 Tribological results illustrated as Stribeck curves for: a) wide (30 µm) and b) narrow (12 µm width) channels for different depths. The marked areas show the range of COF for small sliding velocities (< 10^{-3} m/s).

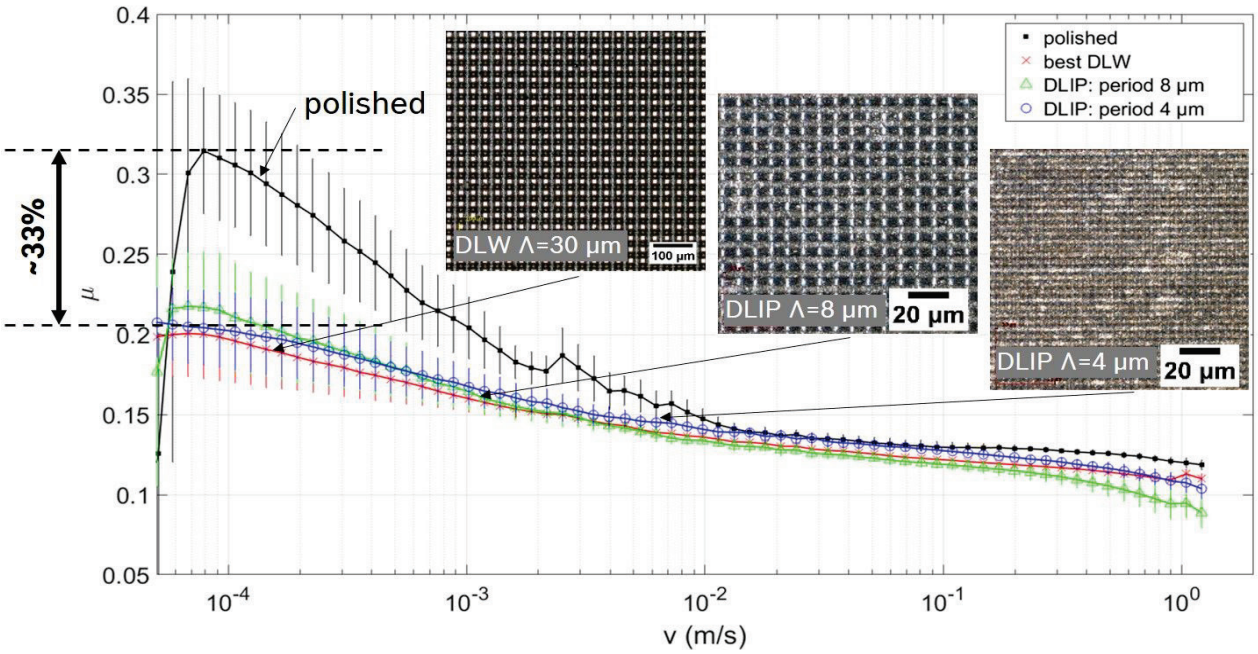

Fig. 6 Tribological evaluation of DLIP structures compared to the best DLW structure (Λ = 30 µm, width of 12 µm and depth of 3 µm).

After that, the tribological performance of the samples with the cross-like DLIP structures was also evaluated. The COF as function of the sliding speed is shown in Figure 6, for the cross-like DLIP patterned samples with Λ = 4 µm and Λ = 8 µm. The performance of these samples was compared with the best DLW-structured sample (Λ = 30 µm, width of 12 µm and depth of 3 µm).

The overall decrease of the COF for these three structures compared to the polished reference is from 0.32 to 0.21 (~33 %). As it can be seen, also for the samples treated with the DLIP method, it was possible to reduce the COF, especially for sliding speeds below 10^{-2} m/s. In addition, the obtained results for the DLIP samples are comparable to the performance of the best DLW treated sample.

However, small difference in the tribological behavior can be observed. For high sliding speeds (1 m/s), the DLIP structure with a spatial period of 8 µm showed a COF of only 0.095. This is about 15 % lower than the best DLW sample. On the contrary, the best DLW textured samples shows a COF 3 % lower for a sliding speed of 10^{-3} m/s, compared to the DLIP structures.

Taking into consideration the long processing times required for DLW, especially when producing textures with small feature sizes (and thus requiring significant efforts to focus the laser light to small spots), DLIP could offer important advantages. For instance, throughputs over 10,000 mm²/min are today possible (and for some materials even up to 1,000,000 mm²/min) [21]. In consequence, future studies will focus on the treatment of 3D parts at high-throughput for determining the limitations of this technology. In this study, only cross-like patterned structures with rectangular arrays were investigated. The advantage of a rectangular patterned shape is an isotropic distribution of the oil. The opposite is true for line-like patterned structures where the spreading velocity of the oil parallel to the surface pattern is higher than perpendicular to them which leads to an anisotropic spreading [22].

4. Conclusions

In this study, the tribological performance of open cross-like structures was evaluated. Two different technologies were utilized for fabricating geometries with very different geometrical characteristics, which are DLW and DLIP.

It the case of the DLW method, the depth of the channels was adapted by controlling the number of overscans (from 3 µm to 24 µm) and the width by using an optical attenuator (from 12 µm to 30 µm). The distance between the channels was also varied between 30 µm and 100 µm.
The smaller patterns were produced using the DLIP method, producing cross-like structures with Λ = 8 µm and Λ = 4 µm spatial periods.

It was found, that all fabricated patterns showed a better tribological performance compared to the polished reference. In particular, the best improvements were observed for sliding speeds below 10^{-2} m/s. Furthermore, samples with smaller geometries showed the best performances (e.g. DLW textures with Λ = 30 µm, width of 12 µm and depth of 3 µm and DLIP treated surface with Λ = 8.0 µm).

The overall reduction compared to the polished reference sample was about 33% for small sliding velocities. This result emphasizes the positive effect of cross-like patterned textures with small feature sizes, especially for the reduction of the COF for low sliding velocities and high pressures.

Since for both, the reference sample and the structured sample, the same martensitic base material is used, this result emphasizes the effect of the laser surface textures and its fluid dynamical properties. Therefore, it is supposed that similar effects of friction reduction can be seen for the same structures on austenitic or ferritic stainless steel. However, if wear is considered, the base material may play an important role.

Acknowledgments

The authors of this work gratefully acknowledge the European Commission for supporting the research activity within the framework of the LASER4FUN project, which has received funding from the European Union's Horizon 2020 research and innovation programme under the Marie Skłodowska-Curie grant agreement No. 675063. The work of A.F.L. is also supported by the German Research Foundation (DFG) under Excellence Initiative program by the German federal and state governments to promote top-level research at German universities. The authors also thank Mr. Gerd Dornhöfer, Mr. Joachim Klima and Mrs. Sarona Frank from the Robert Bosch GmbH for the fruitful discussions.

References

[1] K. Holmberg, P. Andersson and A. Erdemir: Tribol. Int., 47, (2012) 221.

[2] W. Baumgartner, F. Saxe, A. Weth, D. Hajas, D. Sigumonrong, J. Emmerlich, M. Singheiser, W. Böhme and J.M. Schneider: J. of Bionic Eng., 4, (2007) 1.

[3] H. Czichos and K. H. Habig: "Tribologie-Handbuch: Tribometrie, Tribomaterialien, Tribotechnik". (Springer-Verlag), (2010). (in German)

[4] R. S. Cowan and W. O. Winer: "Machinery Diagnostics". In Tribologie-Handbuch, (2015) 697.

[5] I. Etsion: Tribol. Lett., 17, (2004) 733.

[6] A. F. Lasagni, D. F. Acevedo, C. A. Barbero and F. Mücklich: Adv. Eng. Mater., 9, (2007) 99.

[7] A. Rosenkranz, T. Heib, C. Gachot and F. Mücklich: Wear, 334, (2015) 1.

[8] C. Zwahr, D. Günther, T. Brinkmann, N. Gulow, S. Oswald, M. Grosse Holthaus and A. F. Lasagni: Adv. Healthcare Mater., 6, (2017) 1600858.

[9] S. Alamri, A. I. Aguilar-Morales and A.F. Lasagni: Europ. Pol. J., 99, (2018) 27.

[10] A. Lasagni, T. Roch, M Bieda, D. Benke and E. Beyer: Proc. SPIE, Vol. 8968, (2014) 89680A.

[11] A. I. Aguilar-Morales, S. Alamri and A. F. Lasagni: J. of Mat. Proc. Techn., 252, (2018) 313.

[12] J. R. Cho, H. W. Lee, J. S. Sohn, G. J. Kim and J. S. Woo: Europ. J. of Mech.-A/Solids, 25, (2006) 914.

[13] H. Bruus: "Theoretical microfluidics", (2008) 346. Oxford university press.

[14] I. Etsion: J. of Tribol., 127, (2005) 248.

[15] D. Braun: "Groeßeneffekte bei strukturierten tribologischen Wirkflaechen", (2015). (in German)

[16] R. Wahl: "Untersuchung des Einflusses von Mikrotexturierungen auf den einsinnigen, oelgeschmierten Gleitkontakt von Stahl-Saphir-Paarungen", (2011), KIT Scient. Publ.. (in German)

[17] J. Bonse, S. V. Kirner, R. Koter, S. Pentzien, D. Spaltmann and J. Krueger: Appl. Surf. Sci., 418, (2017) 572.

[18] R. Stribeck: Zeitschrift des Ver. Deutscher Ing., 46, (1902) 1341. (in German)

[19] C. Gachot, A. Rosenkranz, S. M. Hsu and H. L. Costa: Wear, 372, (2017) 21.

[20] A. F. Lasagni, T. Roch, J. Berger, T. Kunze, V. Lang and E. Beyer: Proc. SPIE, Vol. 9351, (2015) 935115.

[21] A. F. Lasagni: Adv. Opt. Techn., 6, (2017) 265.

[22] P. G. Gruetzmacher, A. Rosenkranz and C. Gachot: Appl. Surf. Sci., 370, (2016) 59.

(Received: July 24, 2018, Accepted: January 5, 2019)